Lasers in Surgery and Medicine 7:300–306 (1987)

Tissue Interactions and Measurement of Ablation Rates With Ultraviolet and Visible Lasers in Canine and Human Arteries

Michele Sartori, MD, Philip D. Henry, MD, Roland Sauerbrey, PhD, Frank K. Tittel, PhD, Donald Weilbaecher, MD, and Robert Roberts, MD

Department of Pathology (D.W.), Section of Cardiology (M.S., P.D.H., R.R.), Baylor College of Medicine, and the Department of Electrical Engineering (R.S., F.K.T.), Rice University, Houston

Ablation rates measured as the depth of tissue excavation per unit time were determined in human and canine aortas subjected to radiation with ultraviolet (UV) excimer (ArF 193 nm, KrF 248 nm, XeF 351 nm) and visible lasers [continuous wave (cw) and 50-ms chopped argon ion, 478 nm–514 nm; pulsed double-frequency Nd:YAG, 532 nm]. For UV and pulsed double-frequency Nd:YAG lasers ablation rates were constant in time and depended linearly on average laser power, but for cw and chopped argon lasers ablation rates varied with irradiation time and were nonlinearly dependent on laser power. In human aortas, atherosclerosis without gross calcification had no influence on ablation rates. Charring and tissue disruption were observed with cw and chopped argon ion, whereas excimer and pulsed Nd:YAG lasers produced only minimal injury to surrounding tissue. We conclude that the determination of ablation rates is useful for the selection of laser wavelengths and power densities applicable to angioplasty and that UV and pulsed visible lasers permit a better control of ablation compared to continuous wave lasers.

Key words: continuous wave laser, pulsed laser, laser ablation rates, laser angioplasty

INTRODUCTION

Ablation of atherosclerotic tissue with laser beams has received considerable attention, but optimal radiation parameters for the effective and safe destruction of atheromatous lesions have not yet been defined [Macruz et al, 1980; Lee et al, 1981; Abela et al, 1982, 1985; Choy et al, 1982a,b, 1984; Geschwind et al, 1984a,b; Ginsburg et al, 1984; Grundfest et al, 1985; Isner et al, 1985; Eugene et al, 1985]. Abela et al [1982] were among the first to show that the effects of laser radiation on vessels were strongly influenced by the wavelength of the light. Linsker et al [1984] and Srinivasan el al [1985] demonstrated that compared to continuous wave (cw) argon ion or cw Nd:YAG laser, excimer laser radiation (ArF, KrF) resulted in less charring and coagulation necrosis, a finding that was confirmed by Grundfest et al [1985] and Isner et al [1985]. More recently, Deckelbaum [1985] has shown that the extent of tissue damage was reduced with pulsed CO_2 laser compared to cw CO_2 laser.

Since a major difficulty in applying lasers to cardiovascular therapy is arterial perforation, it would seem important to assess in quantitative terms how changes in laser parameters such as wavelength, pulse width, and power density influence the amount of tissue removed per unit of time and the extent of laser injury to surrounding tissue [van Gemert et al, 1985; Welch et al, 1985]. In this study, we determined ablation rates for different lasers applied under well-defined experimental conditions. Results suggest that compared to cw lasers, pulsed lasers have the potential for a better control of tissue ablation. In addition, they show that pulsed lasers in the UV range are more effective than those in the visible range for the removal of tissue.

MATERIALS AND METHODS

Materials

Segments of thoracic and abdominal aorta from 12 mongrel dogs, weighing between 18 and 22 kg, were

Accepted for publication April 17, 1987.

Presented in part at the 58th Session of the AHA, Washington, DC, November, 1985.

Address reprint requests to Michele Sartori, MD, Cardiology, Suite F-905, The Methodist Hospital, 6535 Fannin Street, Houston, TX 77030.

cleaned of periadventitial tissue and opened longitudinally. A caliper accurate to the 0.01 mm was used to select segments measuring 0.9–1.1 mm in thickness.

Human aortas were obtained from fresh cadavers (<6 hr postmortem) and prepared similarly.

Experimental Setup

The experimental setup used in our study is shown in Figure 1. The laser beam was focused on the tissue with a calcium fluoride lens of 25-cm focal length. The laser beam size at the level of the surface of the tissue was determined by measuring the diameter of the spot burned by the laser in a developed photographic paper. Measurements of beam size were also made with an optical slit that was moved stepwise through the focus of the lens. There was excellent agreement between the two methods, and spot sizes of about 0.3-mm diameter were typically obtained in the focus. The energy of the laser beam at the spot site was measured with the aid of an energy meter connected to a storage oscilloscope (Tektronix, model 7834) before every set of experiments.

The lasers used in this study were an excimer laser, an argon ion laser, and a pulsed double-frequency Nd:YAG laser. The excimer laser was a Lambda Physik EMG 101 Model operated on three rare gas fluoride transitions: argon fluoride, krypton fluoride, and xenon fluoride. The argon laser (HGM Model 8) was used in the cw mode and in a interrupted mode (pulse duration 50 ms) referred to as "chopped" mode. The pulsed double-frequency Nd:YAG laser (Quantronix) was chosen because it exhibits a wavelength (532 nm) that is similar to the wavelength of the argon laser (478–514 nm) and a pulse width (7 ns) comparable to the pulse duration of the excimer laser (12 ns).

Arterial segments (n = 102) 3–4 cm long were isolated from dog or human aortas. The segments were mounted on a frame perpendicular to the path of the laser beam and positioned at the focal point of the calcium flouride lens. To expose serially equidistant areas of the sample to the laser, the frames were mounted on a micropositioner. Light transmission through the sample was detected with an energy meter, the output of which was monitored with a storage oscilloscope (Fig. 1). The perforation time was measured as the interval between the onset of radiation and the occurrence of maximal energy transmission.

Measurement of Ablation Rates

The shape of the cross section of the craters in the tissue in direction of the laser radiation was in all cases nearly rectangular; ie, the volume of the craters was almost cylindrical (Fig. 2). Therefore, the ablation R, defined as depth of tissue ablation per unit time, is proportional to the amount of material removed from the

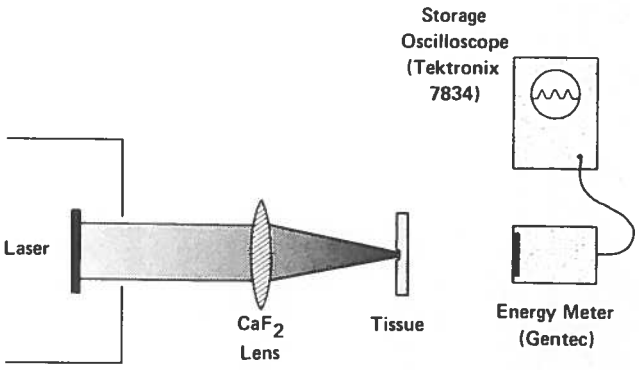

Fig. 1. Experimental setup: The laser beam was focused on the intimal surface of the tissue. An energy meter triggered by the laser and connected to an oscilloscope was placed behind the tissue in the path of the beam. The time from the starting of the radiation to the maximum output signal was defined as time to perforation (T_p).

tissue. The ablation rate was determined by two different methods. With the first method, the arterial wall was completely perforated and R was determined by dividing the known thickness of the samples by the perforation time (T_p). For cw and chopped argon lasers, R was measured first with the minimum power density required to produce perforation within 60 s. For pulse Nd:YAG and excimer lasers, T_p and R were determined at energy densities of 25, 50, 75, and 100 mJ/mm^2 and repetition rates of 10, 20, and 40 Hz. The perforation time and the ablation rate for a given set of radiation parameters were determined from an average of three to five experiments and expressed as means $\pm$ 1 SD.

The second method relied on the morphometric measurement of the depth of nontransmural craters, R being measured as the ratio between crater depth and time of irradiation. In these experiments, power density (7 W/mm^2 for argon ion laser), and energy density and repetition rate for excimer and pulsed Nd:YAG lasers (75 mJ/mm^2 per pulse $\times$ 5 Hz = 0.375 W/mm^2) were kept constant, whereas the time of tissue radiation was varied. Calculation of R by two independent methods allowed us to assess the reliability of our measurements.

Structural Analyses

At the end of the experiments and without dismounting the preparations, the arterial samples were fixed in 10% formalin. The fixed tissue was embedded in paraffin and sectioned through the plane of the lesions. Five-micron-thick sections were stained with hematoxylin-eosin and examined by light microscopy. The dimensions of the craters and of cross-sectional atherosclerotic lesion areas were determined on microphotographs using a computerized planimeter (Digisonics Model-1912) as described by Davis et al [1985].

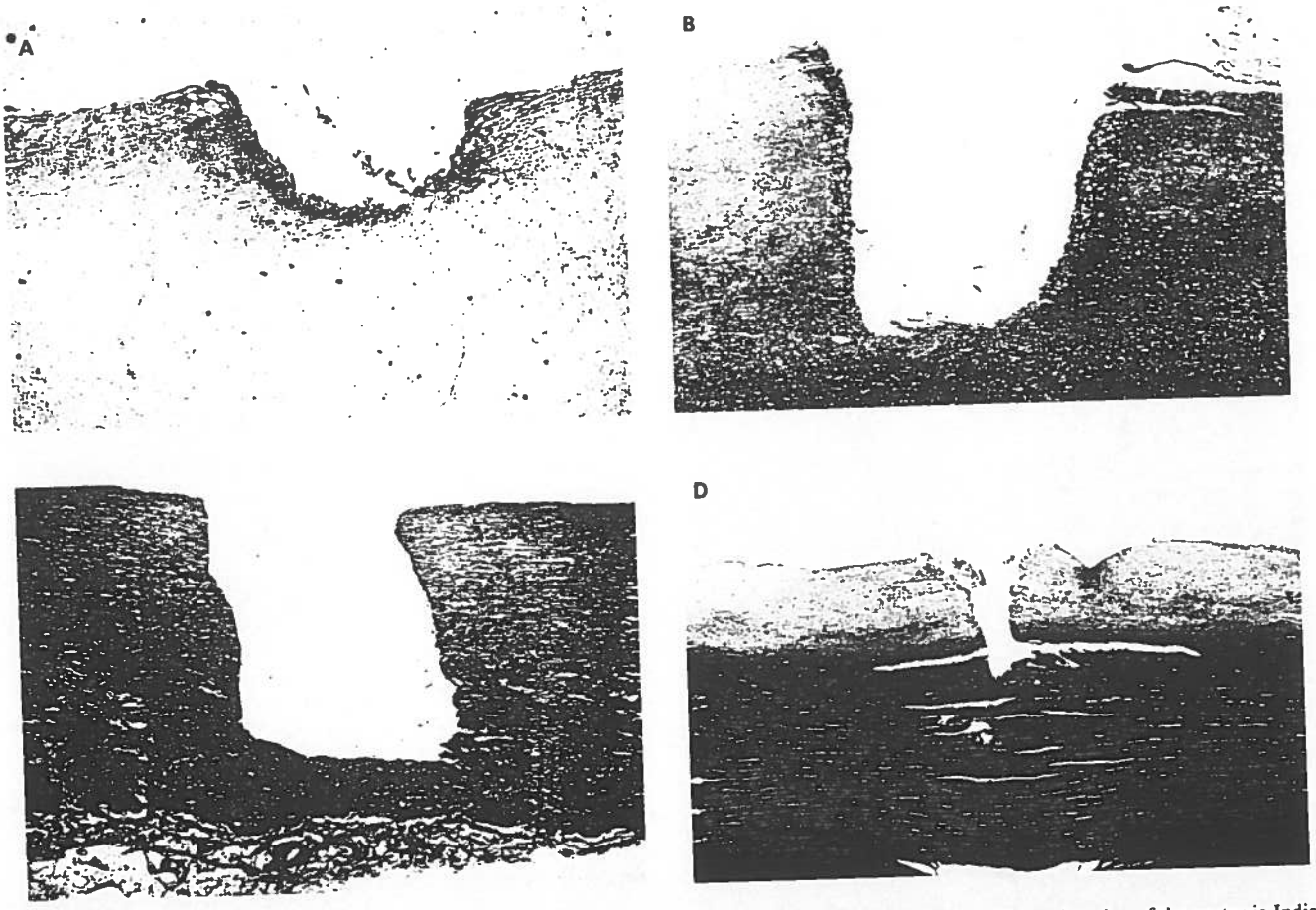

Fig. 2. Craters obtained in atherosclerotic human aortas with different lasers (10 × 8.4). **A**: cw argon. There is extensive charring and tissue disruption at the edges of the crater. **B**: Chopped argon ion. Charring and injury are less than with cw argon. **C**: KrF excimer. The margins of the crater are very regular, and there is no charring or disruption of tissue. The black rim at the edge of the crater is India ink for microscopic retrieval for the site of irradiation (See Materials and Methods). **D**: Pulse double frequency Nd:YAG. No charring is present, but clefts of tissue disruption are produced at the periphery of the crater. The black rim of the edge is in India ink.

RESULTS

Qualitative Observations

With power densities sufficient to produce tissue ablation, irradiation with the cw argon laser resulted in extensive areas of charring surrounded by coagulation necrosis and tissue disruption at the periphery of craters (Fig. 2A). Only a rim of 10–50 μm of charring and tissue disruption was found with the chopped argon laser (Fig. 2B). In contrast, with excimer lasers at 193, 248, and 351 nm, light microscopy visualized no charring or tissue disruption (Fig. 2C).

There was no coagulative necrosis or charring in craters produced by pulsed double-frequency Nd:YAG. However, 10–50-μm wide and 100–500-μm long clefts were seen at the bottom of the craters (Fig. 2D).

Quantitative Results

CW and chopped argon. The relationship between power and tissue penetration of the cw argon laser in the dog aorta is illustrated in Figure 3. Up to a power density of 12 W/mm^2, no ablation occurred after 60 seconds. However, with only minor increases in power density to 13 W/mm^2 a substantial crater depth (150 μm) was created, and with a further minor increase to 14 W/mm^2 perforation occurred (Fig. 3A). When the power density was held constant at 14 W/mm^2, no ablation was observed with irradiation times of up to 57 s (Fig. 3B). Yet, a small prolongation of the irradiation to 59 s produced a 500-μm-deep crater, and a further prolongation to 60 s resulted in the perforation of 1,000-μm-thick vessel walls. A similar phenomenon was observed with the argon laser in the chopped mode (50-ms pulses). Thus, in these experiments with cw and chopped argon lasers there was an abrupt change from no effect to maximal effect (perforation) with relatively minor increases in laser power (Fig. 3A) and total energy delivered (Fig. 3B). This phenomenon is further illustrated in Figure 3C: the perforation time is 60 s at a power density of 14 W/mm^2,

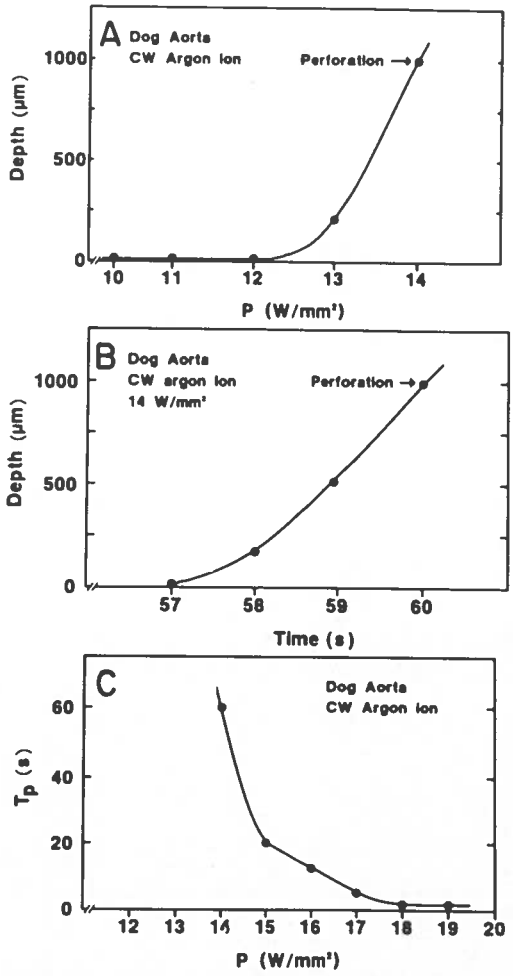

Fig. 3. Crater depth for cw argon ion laser in dog aortas as a function of power density and time. Small increments of power density produce large differences in crater depth (A). At a constant power density of 14 W/mm^2, ablation starts only after 57 s (B), after which perforation is quickly produced within 3 s. With a slightly increased power density of 17 W/mm^2, ablation starts without delay and perforation is achieved within 5 s (C)

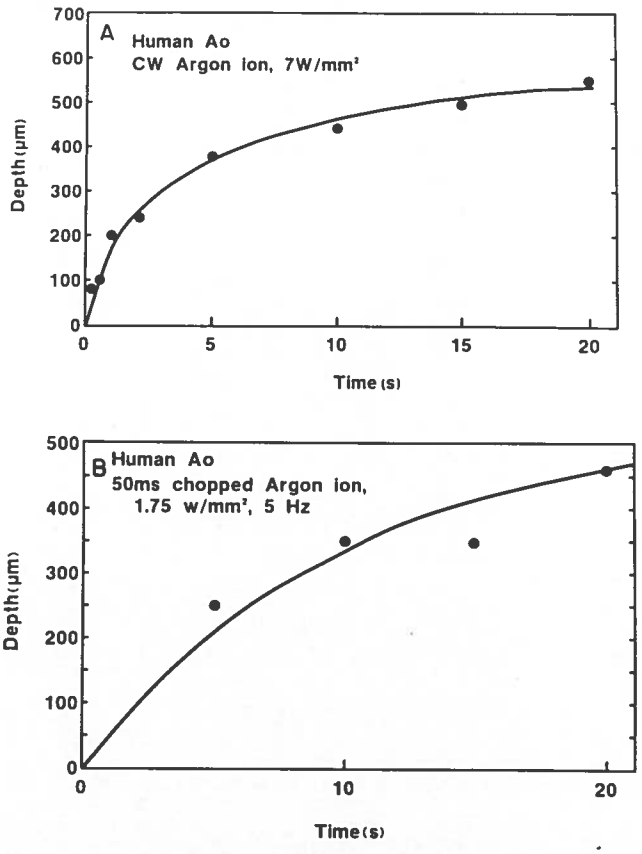

Fig. 4. Crater depth for argon ion laser in human aortas as a function of time. A: cw argon. B: Chopped argon (50 ms, 5 Hz). The crater depth and therefore the ablation rate progressively decrease with time of irradiation.

but decreases to 3 s with an increase in power density of less than 20%. This shows that the ablation rate with the cw argon laser is not linearly dependent on the product of power density and time, ie, energy density.

In human aortas, ablation occurred at lower power densities compared to dog aortas. Ablation rate was calculated by measuring crater depth obtained with various irradation times at a constant power density of 7 W/mm^2. Crater depth did not increase linearly with time, and R decreased with increasing irradation times (Fig. 4). The ablation rate was 120 μm/s for the first 2 s and approximately 15–20 μm/s after 5 s of radiation. In the chopped mode with a power of 1.75 W/mm^2, the initial R value was 35 μm/s and declined with time.

Excimer and pulsed Nd:YAG. Effects of UV pulsed lasers on dog aortas are shown in Figure 5. The crater depth produced by the lasers at a constant power density and repetition rate is plotted as a function of the irradiation time. In contrast to the argon laser, crater depth (d) was proportional to the duration of exposure to irradiation (t). Thus, the slopes of the straight lines representing the ablation rates (R = d/t) were independent of d and t. Similarly, with pulsed Nd:YAG crater depth increased linearly with time when power density and repetition rate were held constant.

By varying power density and/or repetition rate of 10, 20, 40 Hz, of the pulsed UV and Nd:YAG lasers, crater depth was found to be proportional to the average laser power density P; ie, the ablation rate R was a linear function of the product of energy density per pulse and repetition rate (Fig. 6):

$$R = A(P - P_{th})$$

where P_{th} is the minimal power density required to effect ablation (power density threshold), and A is a constant

depending on the laser wavelength and the laser pulse duration. Values of A measured with the perforation time and morphometric methods were in good agreement. Values of P_{th} were identical. The threshold power density increased with increasing wavelengths (Table I). With the XeF and double-frequency Nd:YAG lasers the power density threshold is indicated by the positive intercepts on the horizontal axes (Fig. 6c,d). Comparing ablation rates at the same average power density of 1 W/mm^2, R values in dog aorta for KrF, Nd:YAG, ArF, and XeF were 100, 70, 13, and 9 μm/s (Fig. 6). Therefore, although Nd:YAG exhibited a threshold effect, it had the second-highest ablation rate. No power density threshold was observed for ArF and KrF within the investigated parameter range. As in dog aorta, the crater depth in human aorta was a linear function of irradiation time for UV (Fig. 7) and visible pulsed lasers. The straight lines obtained in both cases demonstrate the constancy of the ablation rates within the laser energy density range tested. Values of ablation rate in human aortas were slightly lower compared to those obtained in canine tissue.

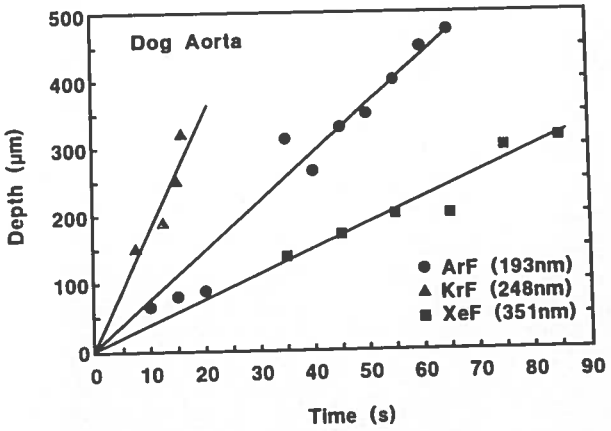

Fig. 5. Crater depth as a function of irradiation time for the three excimer wavelengths investigated in dog aorta. Every point represents the average depth of 3–5 craters produced with a constant energy density of 0.375 W/mm^2. The depth of the craters increases linearly with time. The slope of the curve represents the ablation rate. The highest ablation rate is obtained with the KrF laser (248 nm).

TABLE I. Values (Means ± 1 SD) of Ablation Constant (A), Power Density Threshold (P_{th}), and Ablation Rate (R) for Excimer (ArF, KrF, XeF) and Pulsed Double-Frequency ND:YAG in Dog Aorta

		Ablation constant (A)				
		$\mu m \cdot mm^2/W \cdot s$			Ablation rate (R)* (μm/s)	
Laser	Wavelength (nm)	T_p	Depth	P_{th} (W/mm^2)	T_p	Depth
ArF	193	13	14	0	13	14
KrF	248	75	37	0	100	37
XeF	351	12	5	0.25 ± 0.15	9	4
Nd:YAG (pulsed)	532	126	—[a]	0.45 ± 0.20	70	—[a]

*R-values refer to those obtained with a power density of 1W/mm^2.
[a]Measurement not performed.

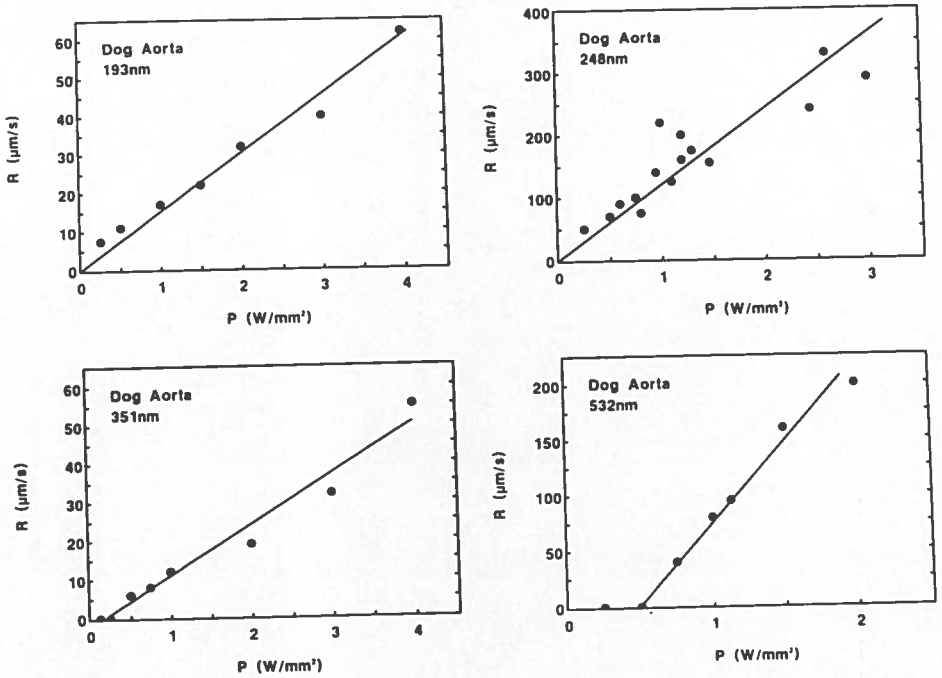

Fig. 6. Ablation rates of pulsed UV and visible lasers in dog aortas. For all wavelengths the ablation rate R is linearly dependent on the average power P.

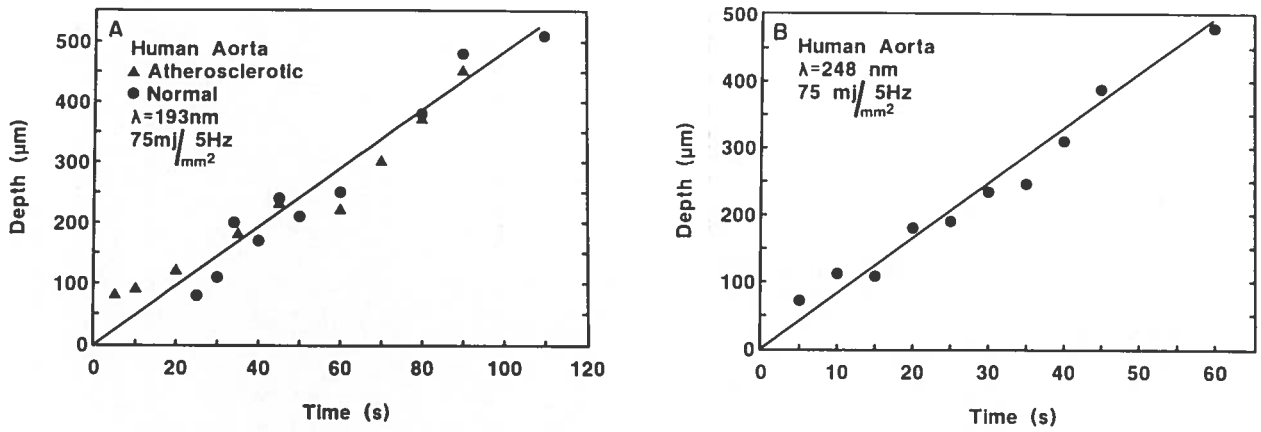

Fig. 7. Crater depths produced by excimer lasers in normal and atherosclerotic human aortas. A: Argon fluoride. B: Krypton fluoride. As in dog aortas, the crater depth depends linearly on the time of irradiation. Crater depth is the same for normal and noncalcified atherosclerotic aortas.

Influence of atherosclerosis. Without gross calcification, R was approximately the same as in normal arteries for all wavelengths. However, in 20 samples exhibiting gross calcification, R-values for all wavelengths were decreased approximately 5–10-fold. No attempt was made to define the quantitative relationship between calcium salts in the tissue and ablation rates.

DISCUSSION

This study shows the potential advantage of pulsed lasers over continuous wave lasers for the controlled ablation of arterial tissue. With pulsed lasers the amount of tissue ablated was augmented in proportion to increases in the repetition rate, the power per pulse, and the duration of irradiation. These linear relationship between ablation and major parameters of laser radiation make ablation predictable and controllable at least under in vitro conditions. In contrast, with cw lasers, ablation rates decreased with time when power was held constant and increased nonlinearly with increasing power. These nonlinear relations along with the production of extensive injury to surrounding tissues make the selection of appropriate irradiation parameters difficult in the cw mode.

The cw and chopped argon lasers are more injurious than the pulsed Nd:YAG, which has a wavelength similar to that of argon. Thus, it appears that short pulse duration and its associated high peak power (pulse energy/pulse duration) are important in determining the pattern of ablation and the damage to surrounding tissue. As pointed out by Deckelbaum et al [1985], the thermal injury of adjacent nontargeted tissues can be avoided when the exposure time for each pulse is shorter than the thermal relaxation time of the irradiated tissue. The nonlinear relation of ablation rate and the extention of injury to surrounding tissue observed with cw lasers may explain the high incidence of perforation reported with the use of cw argon laser [Abela et al, 1985; Isner et al, 1985].

In the cw mode a visible wavelength such as argon ion interacts with tissue through thermal effects. In the nonatherosclerotic white dog aorta, the blue-green light of the argon laser is reflected and a relatively long time is required to reach the temperature threshold at which ablation starts. However, once irradiation time or power are sufficient to produce an elevation in temperature high enough to change the absorption properties of the surface, ablation proceeds rapidly. The human aorta differs from the canine aorta in that it very frequently exhibits atherosclerotic changes associated with the accumulation of argon-laser-absorbing pigments such as carotenoids and tetrapyrrols. The pigmented intima eliminates the initial light reflection, a process that may account for lower ablation threshold and for the linear relation between energy and ablation during the first 5 s of irradiation. The linearity persists until fragments of carbonized tissue accumulating inside of the crater or fragmentation of the pigments decelerate ablation.

Despite the different effects produced by cw and nanosecond pulsed lasers, it should not be construed that wavelength is unimportant. The very low power density threshold exhibited by excimer wavelengths indicates that UV lasers are better absorbed by arterial tissues than pulse Nd:YAG laser. Furthermore, tissue disruption as evidenced by clefts at the bottom of craters after radiation with pulsed Nd:YAG, was not present after irradiation with excimer. Whether such differences are due to a predominance of photochemical over photothermal or photoacoustic effects in the UV range will need further evaluation. Although these findings may suggest that UV

lasers are preferable for microsurgical application, it remains to be demonstrated which type of pulse laser will be most useful for laser angioplasty in the intact organism. In vivo, other factors such as the delivery of UV light through fiberoptic systems may become important. The choice of the wavelength for laser angioplasty depends on the availability of optical fibers able to convey peak power well above ablation threshold. Studies comparing transmission of UV and pulsed visible lasers (such as pulsed argon and Nd:YAG) in air and blood are needed. Irradiation with short high power pulses and the use of dosimetry devices for the controlled delivery of light such as those recently reported by Cothren et al [1986] may be important steps towards avoiding vessel perforation.

Ablation rates (R); ablation constants (A); and power density thresholds (P_{th}) for ArF, KrF, XeF and pulsed frequency-double Nd:YAG lasers calculated in this study with two independent methods were in good agreement. The linear relation between crater depth and irradiation time for excimer laser confirms previous reports by Linsker et al [1984] and Grundfest et al [1985]. The different ablation rates calculated from their results may be explained on the basis of the different excimer wavelengths (XeCl, 308 nm) and pulse durations used in their experiments.

In summary, the results of this study demonstrate that the relationship between energy density and ablation rate is linear for pulsed lasers but nonlinear for cw lasers. The nonlinear relationship in the case of cw lasers may explain the difficulty in controlling tissue ablation and avoiding vascular perforation with this type of laser. In contrast, the linear relationship observed with pulsed lasers should permit a controlled and precise ablation necesary for safe laser angioplasty.

ACKNOWLEDGMENTS

The excellent assistance of Mrs. Winifred Boyce in preparing this manuscript and the help of James Hooten in performing the experiments are greatfully acknowledged.

REFERENCES

Abela GS, Normann S, Cohen D, Feldman RL, Geiser EA, Conti CR: Effects of carbon dioxide, Nd-Yag and argon laser radiation on coronary atheromatous plaques. Am J Cardiol 50:1199–1205, 1982.

Abela GS, Normann SJ, Cohen DM, Frausini D, Feldman RL, Cres F, Fenech A, Pepine C, Conti R: Laser recanalization of occluded atherosclerotic arteries in vivo and in vitro. Circulation 71:403–411, 1985.

Choy DSJ, Stertzer SH, Rotterdam HZ, Sharrock N, Kaminow IP: Transluminal laser catheter angioplasty. Am J Cardiol 50: 1206–1208, 1982a.

Choy DSJ, Stertzner SH, Rotterdam HZ, Bruno MS: Laser coronary angioplasty: Experience with 9 cadaver hearts. Am J Cardiol 50:1209–1211, 1982b.

Choy DSJ, Stertzer SH, Myler KK, Marco J, Fourinal G: Human coronary laser recanalization. Clin Cardiol 7:377–381, 1984.

Cothern RM, Kittrell C, Hayes GB, Willett RL, Socks B, Malk EG, Emsen RJ, Bott-Silverman C, Kramer JR, Feld MS: Controlled light delivery for laser angiosurgery. IEEE J Quantum Electron QE22:4–7, 1986.

Davis R, Glagov S, Zarius CK: Role of acid lipase in cholesteryl ester accumulation during atherogenesis. Atherosclerosis 55:205–215, 1985.

Deckelbaum LI, Isner JM, Donaldson RF, Clarke RF, Labliberta S, Aharon AS, Berstein JS: Reduction of laser-induced pathologic tissue injury using pulseol energy delivery. Am J Cardiol 56:662–667, 1985.

Eugene J, McColgan SJ, Pollock ME, Hammer-Wilson M, Moore-Jeffries EW, Berns MW: Experimental atherosclerosis treated by argon ion and Nd-YAG laser endarterectomy. Circulation 72:II-200, 1985.

Geschwind H, Boussignac G, Teisseire B, Berihevem N, Becquemin JP, Gaston A: Laser angioplasty in cadaver coronary artery stenosis. Eur Heart J 5:172, 1984a.

Geschwind H, Boussignac G, Teisseire B: Transluminal laser angioplasty in men. Circulation 70:II-298, 1984b.

Ginsburg R, Kim S, Guthauer D, Toth J, Mitchell RS: Salvage of an ischemic limb by laser angioplasty: Description of a new technique. Clin Cardiol 7:54–58, 1984.

Grundfest WS, Litvack F, Forrester JS, Goldenberg TS, Swan HJC, Morgenstern L, Fishbein M, McDermind S, Rider DM, Pecole TJ, Laudenslager JB: Laser ablation of human atherosclerotic plaque without adjacent tissue injury. J Am Coll Cardiol 5:929–933, 1985.

Isner JM, Donaldson RF, Funai JT, Deckelbaum LI, Pandian NG, Clarke RH, Konstam MA, Salem DN, Bernstein JS: Factors contributing to perforations resulting from laser coronary angioplasty: Observations in intact human post-mortem preparations of intraoperative laser coronary angioplasty. Circulation 72:II-191, 1985.

Lee G, Ikeda RM, Kozine J, Mason DT: Laser dissolution of coronary atherosclerotic obstruction. Am Heart J 102:1074, 1981.

Linsker R, Srinivasan R, Wynne JJ, Alonso DR: Far-ultraviolet laser ablation of atherosclerotic lesions. Lasers Surg Med 4:201–206, 1984.

Macruz R, Martius JRM, Tupinambas AS, Lopes EA, Vargas H, Pena AF, Caralho VB, Armelian E, Decourt LV:Possabilidades terapenticas do raio laser em atheromas. Argent Bras Cardiol 34:9, 1980.

Srinivasan R, Braren B, Seeger D, Trokel S, Krueger RR: Comparative study of the photochemistry of the cutting (etching) of a synthetic polymer and bovine cornea by excimer laser radiation. Conf Lasers Elec Tr Opt (CLEO) WL2:102–105, 1985.

Van Gemert MJC, Schets GACM, Stassen EG, Bonmer JJ: Modeling of (coronary) laser-angioplasty. Lasers Surg Med 5: 5:219-234, 1985.

Welch AJ, Vevario JW, Pearce JA, Hayes LJ, Motamedi M: Effect of laser radiation on tissue during laser angioplasty. Lasers Surg Med 5:251–264, 1985.